A hybrid finite-difference method for global waveform modeling

M. Treml[1], H. Igel[1], G. Jahnke[2], T. Nissen-Meyer[3] und E. Garnero[4]

1. Dept. of Earth and Environmental Sciences, Ludwig-Maximilians-Universitiät München, Germany
2. Seismic Data Analysis Center at BGR, Stilleweg 2, D-30655 Hannover, Germany
3. Department of Geosciences, 312 Guyot Hall, Princeton University, Princeton, NJ, USA.
4. Dept. of Geological Sciences, Arizona State University, Tempe AZ, USA

Abstract

A new, hybrid finite-difference (FD) method for 3-D global wavefield modeling is presented. It enables high-frequency studies of wavefield effects of confined 3-D structures, such as plumes, on a teleseismic wavefield that has travelled through an axi-symmetric background model.
For such 3-D wavefield studies full-3-D waveform modeling methods can be used (e.g. Komatitsch and Tromp [2002]) which is however restricted to low frequencies due to still existing limitations in computer power. To overcome this problem, hybrid approaches have been developed (e.g. Wen and Helmberger [1998]; Wen [2002]; Capdeville *et al.* [2002, 2003]), combining existing methods with the aim of extending the frequency range of simulations. We present a method that combines a global axi-symmetric FD algorithm with one for a confined 3-D spherical section. The teleseismic global wavefield through an axi-symmetric, or standard 1-D model can be calculated with a 2-D method that takes advantage of its axi-symmetry and thus correctly takes into account 3-D geometrical spreading behavior. It is passed to a 3-D spherical section that can include an arbitrary, confined 3-D structure implemented in the same background model as was used for the axi-symmetric domain In this spherical section the 3-D wave equation is solved allowing for studying the 3-D wavefield effects of the structure.
The method is applied to a plume model that is placed in PREM at an epicentral distance of 90 degrees. The 3-D effects of the plume on the SH-wave is examined including conversions to P and SV waves.

Introduction

Numerical modeling of global wave propagation is of eminent importance for modern seismology. Synthetic seismograms of standard 1-D Earth models such as IASP91 (KENNETT AND ENGDAHL [1991]) or PREM (DZIEWONSKI AND ANDERSON [1981]) serve as references.Modeling the effects of specific structures in the Earth such as subduction zones, plumes or ultra-low velocity zones at the core mantle boundary on the seismic wavefield and understanding how these effects can be used to image these structures is another important field for numerical modeling. Moreover, full-waveform inversion techniques are under development (adjoint method, time-reversal imaging, e.g., TROMP *et al.* [2005]) and will be feasible in future due to increasing computer power and the existence of adequate 3-D global wavefield modeling methods. This will open up a new era in imaging the Earth's interior and in exploiting the entire information that is delivered with seismograms.

To date, a variety of computer programs and methods are available to generate synthetic seismograms, the classical and most popular ones being the reflectivity method (FUCHS AND MÜLLER [1971]), the WKBJ-method (CHAPMAN [1978]), and normal mode summation (e.g. CAPDEVILLE *et al.* [2000]).

Complete methods for numerical wavefield modeling can achieve arbitrary accuracy but can require enormous computational resources. They solve the partial differential equations of the full wavefield.Direct methods include the Finite-Difference method, the Finite-Element method, the Finite-Volume method, pseudospectral methods (such as the Fourier and the Chebychev method), and the Spectral Element method.

A hybrid finite-difference method

This section briefly summarizes the finite-difference method, motivates the use of hybrid methods for global wave propagation, reviews finite-difference methods for wave propagation in spherical media and describes the construction of a hybrid finite-difference method from two of the approaches.

The finite-difference method

Finite Differences (FD) have widely been used to numerically propagate seismic waves. Comprehensive reviews of the method and their application to seismic wave propagation have been given recently by MOCZO *et al.* [2004] in the framework of the European SPICE project or will be published in near future (MOCZO *et al.* [2006]). The major advantage of the method is its relative simplicity and the use of local operators, allowing for simple model splitting and thus easy parallelization of the algorithms.

Several FD-codes have been developed by IGEL and co-workers (e.g., IGEL [1993], IGEL AND WEBER [1995], IGEL AND WEBER [1996], IGEL AND GUDMUNDSSON [1997], THOMAS *et al.* [2000]) and served as a basis for further developments. For example, a Cartesian 3-D FD code was developed by STRASSER [2001] for applications on wave propagation through mantle plumes at regional distances. This work was promising since it showed observable effects of plumes consistent with the work by TILMANN *et al.* [1998]. It also demonstrated the need to use spherical geometry when one wants to study seismic effects of plumes at larger distances.

Most FD approaches are based on the velocity stress formulation (VIRIEUX [1986]) combined with a staggered grid. Therefore, both will be explained in the following. The velocity-

stress formulation of the seismic equation of motion for an elastic anisotropic medium with a moment tensor and single force excitation reads (e.g. MOCZO *et al.* [2006])

$$\rho \frac{\partial v_i}{\partial t} = \nabla_j (\sigma_{ij} + M_{ij}) + f_i \tag{1}$$

for generalized version of Newton's second law (action principle), and

$$\frac{\partial \sigma_{ij}}{\partial t} = c_{ijkl} \frac{\partial \varepsilon_{kl}}{\partial t} \tag{2}$$

for the generalized Hooke's law that assumes that the elastic properties of the medium are constant in time and describes the elastic behavior of the material. The elasticity tensor c_{ijkl} contains 81 components, of which only 21 are independent due to the symmetry of the stress and the strain tensors and energy conservation constraints. For the case of an isotropic medium it reduces to the two elastic moduli, Lamé's second constant λ and the shear modulus μ. The moment tensor M_{ij} represents the double couple forces, single sources are given by f_i.

The principle of the FD method for solving these two partial differential equations lies in the approximation of the spatial functions by truncated Taylor series. For the velocity v this reads

$$v(x + \Delta x) = v(x) + \partial_x v(x) + \frac{\Delta x^2}{2!} \partial_x^2 v(x) + \dots \tag{3}$$

leading – for example, for a centered difference scheme – to

$$v(x + \Delta x) \approx \frac{v(x + \Delta x) - v(x - \Delta x)}{2 \Delta x} \tag{4}$$

for the second order approximation of the first derivative. The approximation error caused by the truncated terms of 3 with respect to 4 is proportional to Δx^2.

To apply finite-differences to the seismic wave equation, it is necessary to discretize the stiffness tensor c_{ijkl}, the density ρ and the wavefield v_i on a spatial grid. To do so most FD methods use a "staggered grid" where the wavefield variables and the material properties are not defined on the same grid points. This reduces the approximation error from Δx^2 to $\frac{\Delta x^2}{2}$ while not requiring more memory.

The time evolution is approximated using the same Taylor series truncation which leads to

$$v(t + \Delta t) \approx v(t) + \frac{\partial v(t)}{\partial t} \Delta t \tag{5}$$

The cycle for solving the wavefield equations consists of updating the velocity values from the neighboring ones, then updating the stress values with the new velocity values and finally extrapolating the values in time using eq. 5.

Modern FD programs mostly use a 4th-order spatial approximation instead of the 2nd-order scheme shown above for the sake of simplicity. Moreover, if not modeling the entire globe, there are unphysical model boundaries leading to artificial reflections. These are avoided using so called "absorbing boundaries", that is, a rim of grid points where the function values are multiplied with an decreasing factor <1. They continuously damp the wavefield towards the model boundaries and this weakens the wave and its reflections from the model boundary such that they do not influence the modeled seismograms.

Finite difference methods for spherical media

When considering wave propagation on a global scale, it is useful to turn to spherical coordinates since the Earth is in first approximation a sphere. When expressing the elastic wave equation (1) in spherical coordinates (r, θ, φ) one obtains (e.g. NISSEN-MEYER [2001]):

$$\rho\frac{\partial v_r}{\partial t} = \frac{\partial \sigma_{rr}}{\partial r} + \frac{1}{r}\frac{\partial \sigma_{r\theta}}{\partial \theta} + \frac{1}{r\sin\theta}\frac{\partial \sigma_{r\varphi}}{\partial \varphi} + \frac{1}{r}(2\sigma_{rr} - \sigma_{\theta\theta} - \sigma_{\varphi\varphi} + \sigma_{r\theta}\cot\theta) + f_r \quad (6)$$

$$\rho\frac{\partial v_\theta}{\partial t} = \frac{\partial \sigma_{r\theta}}{\partial r} + \frac{1}{r}\frac{\partial \sigma_{\theta\theta}}{\partial \theta} + \frac{1}{r\sin\theta}\frac{\partial \sigma_{\theta\varphi}}{\partial \varphi} + \frac{1}{r}([\sigma_{\theta\theta} - \sigma_{\varphi\varphi}]\cot\theta + 3\sigma_{r\theta}) + f_\theta \quad (7)$$

$$\rho\frac{\partial v_\varphi}{\partial t} = \frac{\partial \sigma_{r\varphi}}{\partial r} + \frac{1}{r}\frac{\partial \sigma_{\theta\varphi}}{\partial \theta} + \frac{1}{r\sin\theta}\frac{\partial \sigma_{\varphi\varphi}}{\partial \varphi} + \frac{1}{r}(3\sigma_{r\varphi} + 2\sigma_{\varphi\theta}\cot\theta) + f_\varphi \quad (8)$$

If we also assume the model to be rotationally symmetric (axi-symmetric) with the $\theta = 0$ line as symmetry axis the equations become invariant with respect to φ. Thus, all derivatives with respect to φ are vanishing. Then it reads (e.g. THOMAS *et al.* [2000]; IGEL AND WEBER [1995]):

$$\rho\frac{\partial v_r}{\partial t} = \frac{\partial \sigma_{rr}}{\partial r} + \frac{1}{r}\frac{\partial \sigma_{r\theta}}{\partial \theta} + \frac{1}{r}(2\sigma_{rr} - \sigma_{\theta\theta} + \sigma_{r\theta}\cot\theta) + f_r \quad (9)$$

$$\rho\frac{\partial v_\theta}{\partial t} = \frac{\partial \sigma_{r\theta}}{\partial r} + \frac{1}{r}\frac{\partial \sigma_{\theta\theta}}{\partial \theta} + \frac{1}{r}(\sigma_{\theta\Theta}\cot\theta + 3\sigma_{r\theta}) + f_\theta \quad (10)$$

$$\rho\frac{\partial v_\varphi}{\partial t} = \frac{\partial \sigma_{r\varphi}}{\partial r} + \frac{1}{r}\frac{\partial \sigma_{\theta\varphi}}{\partial \theta} + \frac{1}{r}(3\sigma_{r\varphi}) + f_\varphi \quad (11)$$

Note that now the P- and the vertical S waves (PSV, first two equations) are decoupled from the horizontal S-waves (SH, last equation). Due to the decoupling of SH- and PSV waves in the axi-symmetric case, they can be treated separately and independent of each other.

On the basis of equations 8 and 11 two main developments of finite-difference codes exist for global wave propagation simulation, the axi-symmetric, and the spherical section approach. For global wave propagation, an axisymmetric SH-wave FD code was developed by CHALJUB AND TARANTOLA [1997] and CHALJUB [2000]), and extended to higher orders by IGEL AND WEBER [1995]. The concept of axisymmetry was transferred to the P-SV case by IGEL AND WEBER [1996] and has been further modified by JAHNKE [2005] with the extension to higher orders and the propagation through the inner core. Since axisymmetric computations are carried out in a 2D domain, these codes allow one to achieve a much higher resolution than with a full 3D domain. Despite the use of 2D domains, this method is capable of accurately reproducing the effects of three-dimensional geometrical spreading. Because of the axisymmetry of the problem, the results can be extended to three dimensions by simply rotating the wavefield around the axis.

The input of axi-symmetric (which includes all 1-D) Earth models such as PREM (DZIEWONSKI AND ANDERSON [1981]), IASP91 (KENNETT AND ENGDAHL [1991]) or AK135 (KENNETT *et al.* [1995]) is adequate for many issues in global seismology and the results give helpful constraints in terms of 1D reference model solutions e.g., for tomography. However, the implementation of sources or regional structures in the Earth require these be extended to rings (or, cylindrical volumes if including the axis) due to the axisymmetry (figure 1). For example, a plume at some epicentral distance is extended to a ring structure with the radius of the epicentral distance; thus no true 3D study of wavefield effects of such an object can be carried out using the axi-symmetric approach on its own.

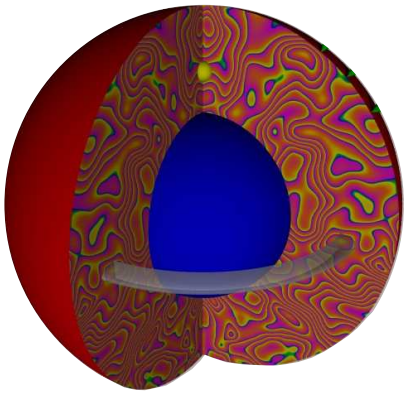

Figure 1: Illustration of axi-symmetry. The source (yellow point) is centered at the axis. The heterogeneous structures along a cut plane through the center are independent of ϕ and therefore ring-like (grey). Figure modified after JAHNKE *et al. [2002].*

Concerning seismic sources, this problem can be overcome by placing a point source at (or technically actually close to the axis. The assumption of a point source still permits progress on many important studies that utilize teleseismic data at high frequencies.

NISSEN-MEYER [2001] developed a 3-D FD method in spherical geometry, however limited to spherical sections to avoid singularities and diminishing grid spacing towards the axis and the center, and applied it to simulate wave propagation through subducting slabs (IGEL *et al.* [2002]). Reflections from the artificial model boundaries are suppressed using absorbing boundary conditions. This method is particularly useful to look at continental scale wave propagation, when the spherical nature of Earth and its effect on the wave field has to be taken into account and lateral heterogeneities have considerable strength (e.g. subduction zones, continental margins, etc.).

In summary, both the axisymmetric approaches as well as the spherical section approach suffer from severe restrictions when applied to global wave propagation through lateral structures such as plumes or subduction zones at teleseismic distances.

In general, it can be stated that for teleseismic wavefield studies of locally confined 3-D structures in a radially symmetric background model, full 3D calculations are a computational waste since the wavefield propagates most of the distance in a radially symmetric Earth model that is more efficiently dealt with using a 2D computational domain or alternative techniques. On the other hand, with the presence of spherical section codes there are tools for computing the regional wavefield effects around 3-D structures. Thus a combination of axi-symmetric and spherical sections approaches towards a hybrid algorithm appears desireable.

The hybrid finite-difference approach

Hybrid methods for global wave-propagation

At present, hybrid methods are a hot topic in computational global seismology since they are able to overcome the drawbacks of the individual methods while combining their advantages. Recently developed hybrid methods for teleseismic lower mantle studies (WEN AND HELMBERGER [1998], WEN [2002], combine 1D and 2D methods (generalized ray theory, 2D-FD simulations, and Kirchhoff theory).

Another approach, closer to the hybrid idea presented and realized within this paper is the combination of the spectral-element method for spherical geometries with normal-mode approaches (CAPDEVILLE *et al.* [2002, 2003]). It couples the normal mode solution for the inner, radially symmetric part of the Earth (the inner and outer core and for 3-D upper mantle studies also the lower mantle) with the SEM for the entire or the upper mantle, respectively. A disadvantage of the method is, that the interface between the domains has to be strictly spherically symmetric, thus precluding the incorporation of effects due to CMB topography or the ellipticity of the Earth (KOMATITSCH AND TROMP [2002]).

Hybrid finite-difference approach

Coming back to the two finite-difference approaches presented in the last section – the axi-symmetric and the spherical section codes – it is evident that there are obvious drawbacks with either of the approaches when attempting to model scattering effects of highly localized 3-D structures (from here on, we will take a plume as an example). In order to overcome these limitations we decided to combine the approaches with the goal of exploiting the long-distance simulation capabilities of the axi-symmetric approach with the complete 3-D solution in a localized region, thereby considerably widening the frequency range that can be modeled with current computer hardware. The idea of this hybrid approach is to calculate the propagation of the wavefield from the source through a axi-symmetric (e.g., 1-D) Earth model over teleseismic distances using the axisymmetric approach. At the distance where the plume is to be modelled the axi-symmetric wavefield is passed to the boundaries of the 3-D spherical section (figure 2) and continues to be calculated in full 3D towards the 3D plume model. Thus, within the 3D-section, true 3D wavefield effects like scattering and refraction can be modelled using an incoming teleseismic wavefield that can up to now not be calculated in 3D for higher frequencies with a reasonable effort.

The lateral extent and position of the 3-D spherical section with respect to the source (the epicentral distance of the target 3D object) can be freely chosen, keeping in mind that close to the polar axis we are approaching singularities in the grid. Thus, centering the 3D section around the equator (e.g. 65-115°) is ideal since the lateral grid spacing within the spherical section is exposed to the least variations. This is an appropriate distance range for many teleseismic studies. At closer distances, the 3D spherical section code may be used alone without excessive computational effort.

An advantage for the hybrid method presented here arises from the fact that for the axi-symmetric case, the SH and the PSV components of motion are decoupled — as mentioned above. For the hybrid method that means that it is possible to combine only one of the two axi-symmetric codes with the 3-D spherical section code and to study the effect of one type of motion alone. This is especially interesting for studying conversions from one type of

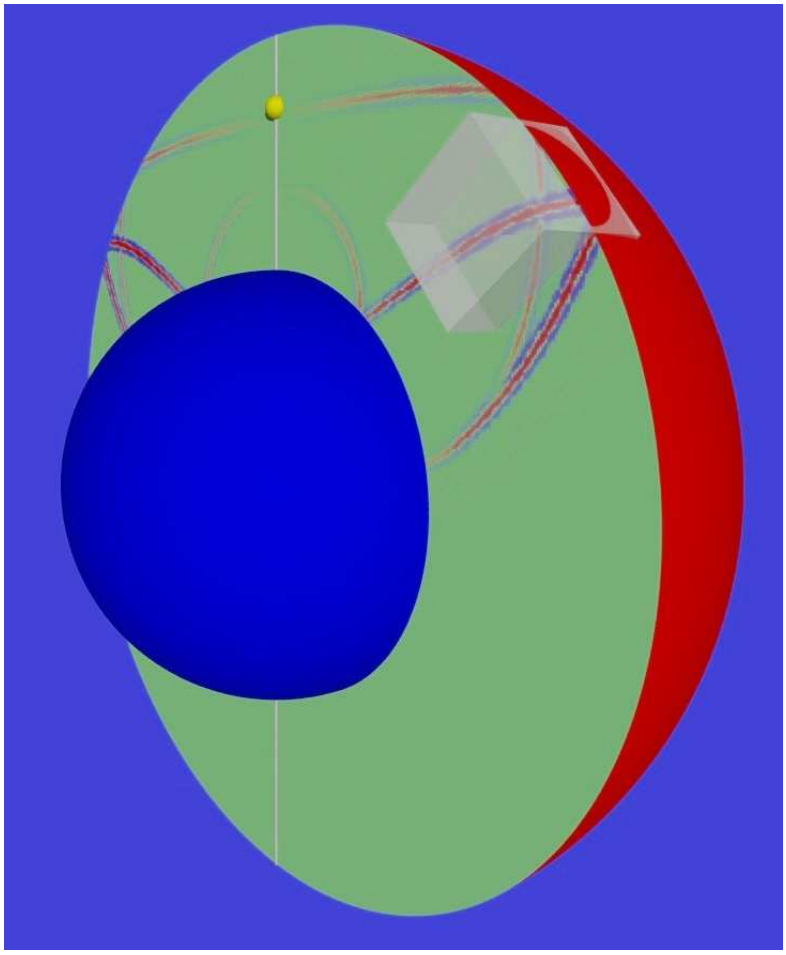

Figure 2: Hybrid axisymmetric/3D-approach. The global wavefield is computed on an axisymmetric 2D-domain with the source centered on the axis. It is then passed to the regional 3D spherical section that is located at some distance and includes the 3D structure of interest.

motion induced by the 3-D structure to the other. An example for this will be shown in the application section.

Even if conceptually simple, care must be taken when combining the two axisymmetric and the spherical section algorithms. In order to guarantee a reliable interplay of the three codes that form the hybrid code it has to be made sure that the grid spacing and the background model are identical, and that the time step as well as the time evolution cycle are synchronized. This is ensured by using a hybrid initialization subroutine for both sub-codes (see fig. 3).

The calculation of wave-propagation in the 3-D section only starts when energy arrives at 10 grid points around the spherical section for the first time. For the serial version of the code this saves a lot of computation time since the wave-propagation over the teleseismic distance is only computed with the fast 2-D axi-symmetric algorithm. This is another advantage of the hybrid concept presented here.

After the 3-D section code is switched on the codes must in each time step run either one after the other or in parallel (for a parallel algorithm) during the time evolution loop

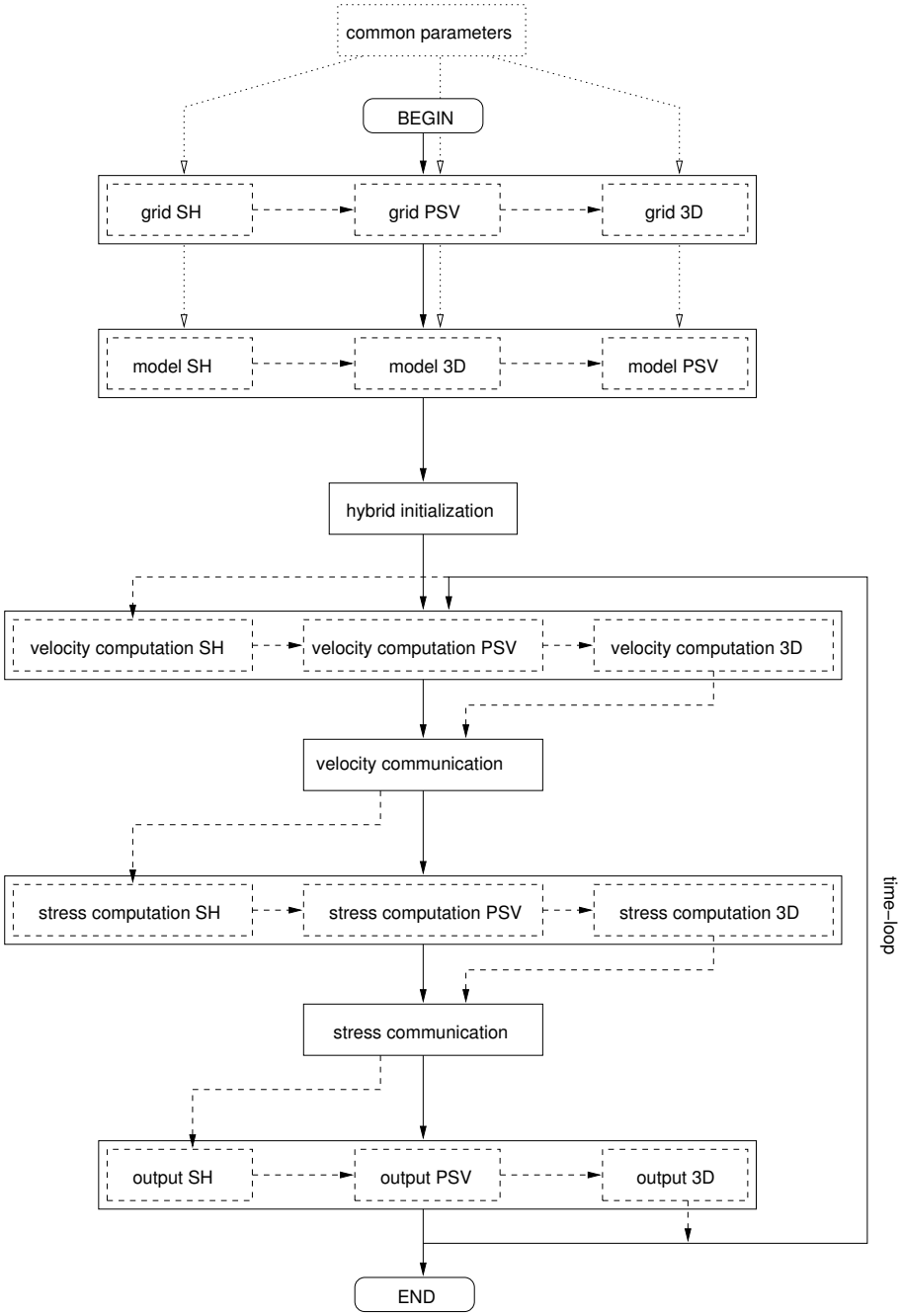

Figure 3: Flowchart of the hybrid code: full lines and boxes represent the program flow of a parallel algorithm, the dahed lines and boxes are for serial execution of the code. Note that not every component (SH, PSV, 3D) has to be switched on. It is possible to run the code omitting either SH or PSV, and the 3-D section (and thus the communication parts) may only be switched on after the first arrival of energy at its edges in order to save computaton time. The subroutines for gridding and model initialization get their parameters from a common parameter file. In the hybrid initialzation part the time step is derived from the stability criterion and the model parameters of all the sub-codes.

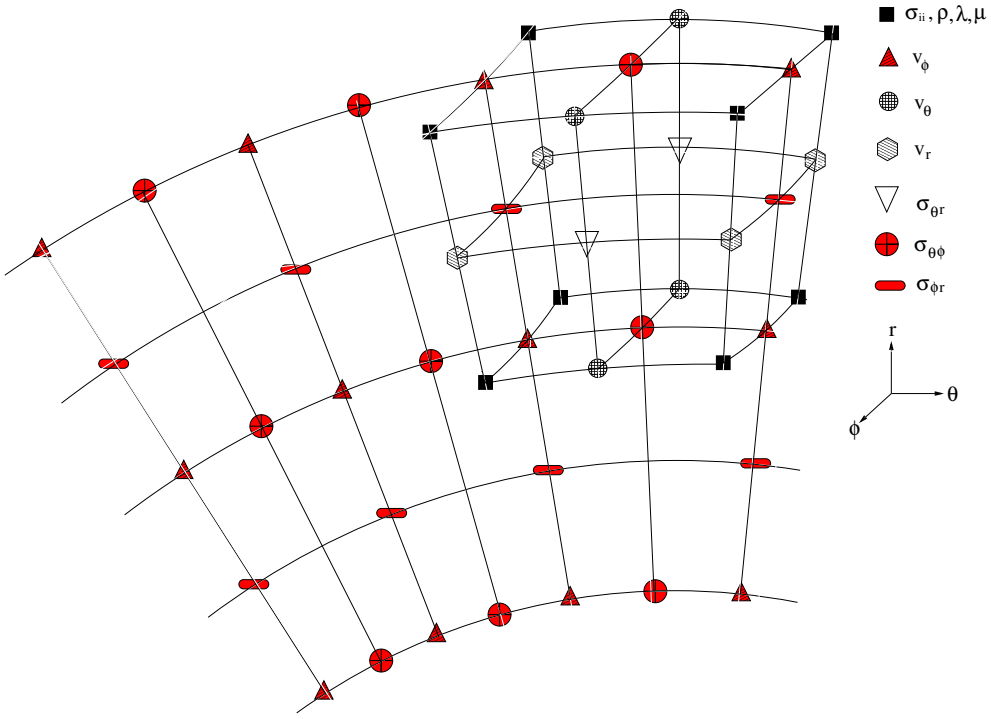

Figure 4: The hybrid grid (example for SH case). Several grid cells of the axi-symmetric SH grid are shown together with one 3D grid cell of the spherical section grid. Different symbols represent grid points with different variable defined there. Red symbols stand for variables that are necessary to define horizontal shear waves.

of the velocity-stress cycle Virieux [1986]. Moreover, the velocity-stress cycle of classical finite-difference codes has to be split into seperate parts for velocity and stress, to enable communication between the axi-symmetric and the 3-D codes after each part (see fig. 3).

The actual heart of the hybrid code is the interface between the axi-symmetric codes for global wave propagation and the regional spherical 3D section. The r and θ coordinates of the gridpoints of the 3D section correspond to (i.e. spatially coincide with) the gridpoints of the axisymmetric grid. For illustration, figure 4 shows the grid cell of the spherical section 3D-FD scheme and its position in the axi-symmetric SH 2D grid. Coupling of the grids and thus of the two codes is done by communication of the wavefield information for the grid points. In order to correctly pass the global wavefield to the 3-D code the first $nop/2$ (nop= operator length) points of the front side and the bottom of the spherical section are set to the corresponding velocity and stress values of the axi-symmetric code. This is done for every time step (and for velocity and stress seperatly) and ensures a continuous flow of the global wavefield into the 3-D box.

As an alternative to the program flow just presented the global axi-symmetric wavefield may also be stored once for all since it does not change for the types of studies for which the hybrid concept presented here is suited. In that case, instead of the execution of the axi-symmetric code(s) the axi-symmetric wavefield has to be read from disk in the communication subroutines. Depending on the actual setup and the disk access speed this might lead to a significant reduction of computation time when carrying out computations with the same configuration but many different models in the 3-D section. This option can be regarded as

using the spherical section code with "boundary conditions" determined by the global wavefield.

As a consequence of this way of coupling the codes the absorbing boundaries of the spherical 3-D code have to be modified. When feeding the axi-symmetric wavefield in the spherical section code at the front and the bottom side, no absorbing boundaries can be used at these sides. In consequence, waves running (back) towards the front end and the bottom of the spherical 3D section are reflected at this feeding-in zone. However, since there are no sources in the spherical section model itself – as it would be usual for FD modeling – and since the main direction of wave propagation is towards the surface and the back end of the section (where an absorbing boundary exists) this is not a severe limitation. Only waves reflected by the plume or the surface or converted waves by the plume might run 'backward' and are thus reflected at the model end. By extending the size of the spherical section in θ- and vertical direction the arrivals of these reflections at the receivers can be delayed such that they will not appear on the seismograms at times were phases of interest show up. Extending the section is not a significant waste of model space because the points that would have been necessary for the absorbing boundaries can be spent for this purpose. Moreover, since it takes twice the time for waves to run to the model and the reflected waves to come back every grid point spent to extend the spherical section increases the delay significantly.

The same reasoning is used to justify circular boundary conditions that are necessary to avoid refractions from the 'loose ends' of the sides of the block, where derivatives can not be calculated due to missing neighbors and absorbing boundaries can not be used either.

The general direction of energy, however, is towards the back side of the block. So from this side the strongest reflections are to be expected. These can be damped away with absorbing boundaries placed at the back-end of the block.

In addition, the restrictions on placing absorbing boundaries only apply to the components that are communicated. Take for example the SH-case. Only SH-energy reflected at the plume is reflected at the communication zone or appears on the other side due to circular boundary conditions. Conversions showing up on other components can run into the absorbing boundaries at all sides.

Verification

Comparison of seismograms produced by the spherical section part of the hybrid code with the ones of the axisymmetric part provides a simple verification of the hybrid method since the axisymmetric code is verified within the COSY project (IGEL *et al.* [1999]), while the accuracy of the spherical section method is assessed by IGEL *et al.* [2002].

If both domains use the same model, the wavefields and thus the seismograms recorded at the surface are supposed to be identical. This comparison is shown in fig. 5, where the first onsets of the SH wave for receivers in both domains are shown together. fThe background model used is the isotropic part of PREM without the crustal layer. For the 105°-extension in the θ-direction, 2 000 grid points are used, and for the vertical direction down to the core-mantle boundary 580 grid points are used. At a distance of about 81° (1545 grid points) the 3-D spherical section grid begins. It extends 350 grid points (18.375°) in the θ-direction (including 50 points for absorbing boundaries). and 250 points (13.125°) in the φ-direction. The 3-D section is discretized with 180 grid points in the vertical direction which corresponds to a depth of about 900 km, thus including the entire upper mantle. Computations were carried out on a 2.8GHz Pentium 4-processor, required 1820MB of RAM and took about 39 hours.

A point source function is used one grid point from the symmetry axis. The source time-function can be arbitrarily chosen, with the possibility to use an impulsive (δ-) source excitation in time, which leads to seismograms that are Green's functions, which can then be convolved with any desired source wavelet. For the seismograms shown, a 20 s two-pole Butterworth low-pass filter for the suppression of numerical noise was used. The waveforms

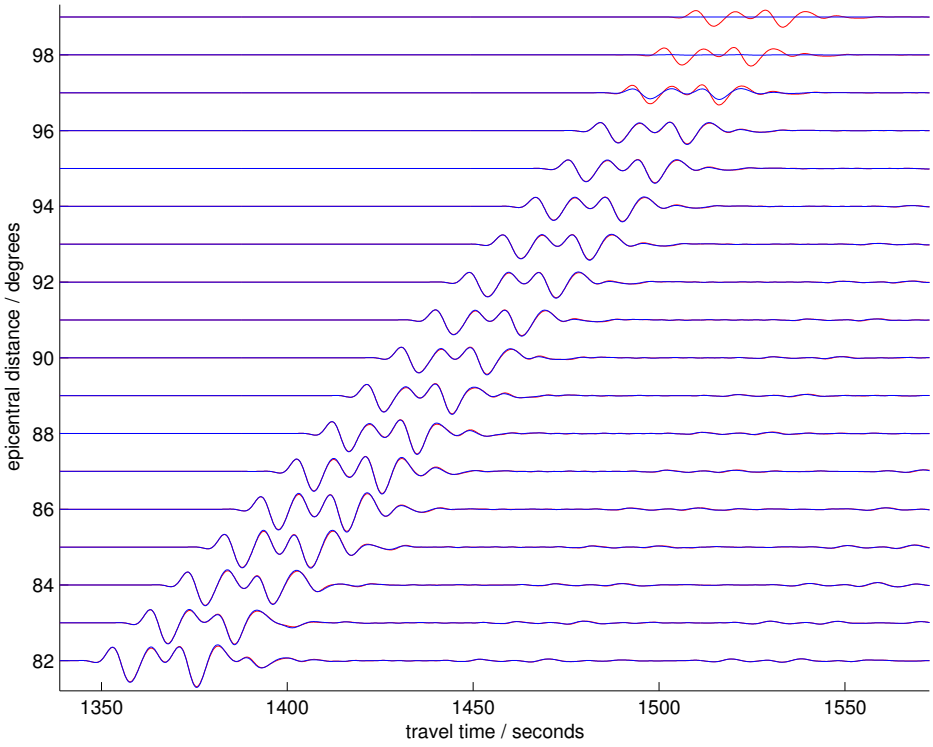

Figure 5: Seismograms for Δ=82-99° epicentral distance calculated with the hybrid code. Both domains, the axisymmetric (red line) and the 3D (blue line), use the PREM model. The direct S_H/ScS_H-wave is shown. Deviations between the seismogram pairs observable from 97° on result from absorbing boundaries that affect the 3D section from this distance on. At 99° on the 3D signal is effectively down at zero amplitude.

are very similar, however, slight differences are observable. These might result from the small differences in the dispersion relation between the two- and the three-dimensional case and would thus be intrinsic to the hybrid method. Apart from that, it can be seen that at higher epicentral distances the seismograms of the spherical section diminish due to the use of absorbing boundaries at the back side of the section.

Application of the hybrid approach

As an illustration of the functionality of the hybrid method, we show an application on a plume at about 90° epicentral distance. Only the axisymmetric SH code is coupled with the spherical section code. This enables us to study conversion from SH to P-SV waves caused by the plume.

The setup is the same as used for fig. 5, only that here, in order to obtain snapshots of the wavefield, a band-limited source spectrum is required. We used 20 s as the dominant

period for for a Gaussian source-time function. The plume at a epicentral distance of 88.75° consists only of a conduit with a radius of 100 km and perturbations of densitity, P-, and S-wavespeed of 10, 15, and 25%, respectively. These relatively high perturbation values were used to enhance the delay due to the plume, because otherwise the deflection of the wavefront would not be visible in the snapshost due to the ratio between wavelength and deflection. Fig. 7 shows the resulting snapshots for all components through different cross-sections through the plume, or at the surface.

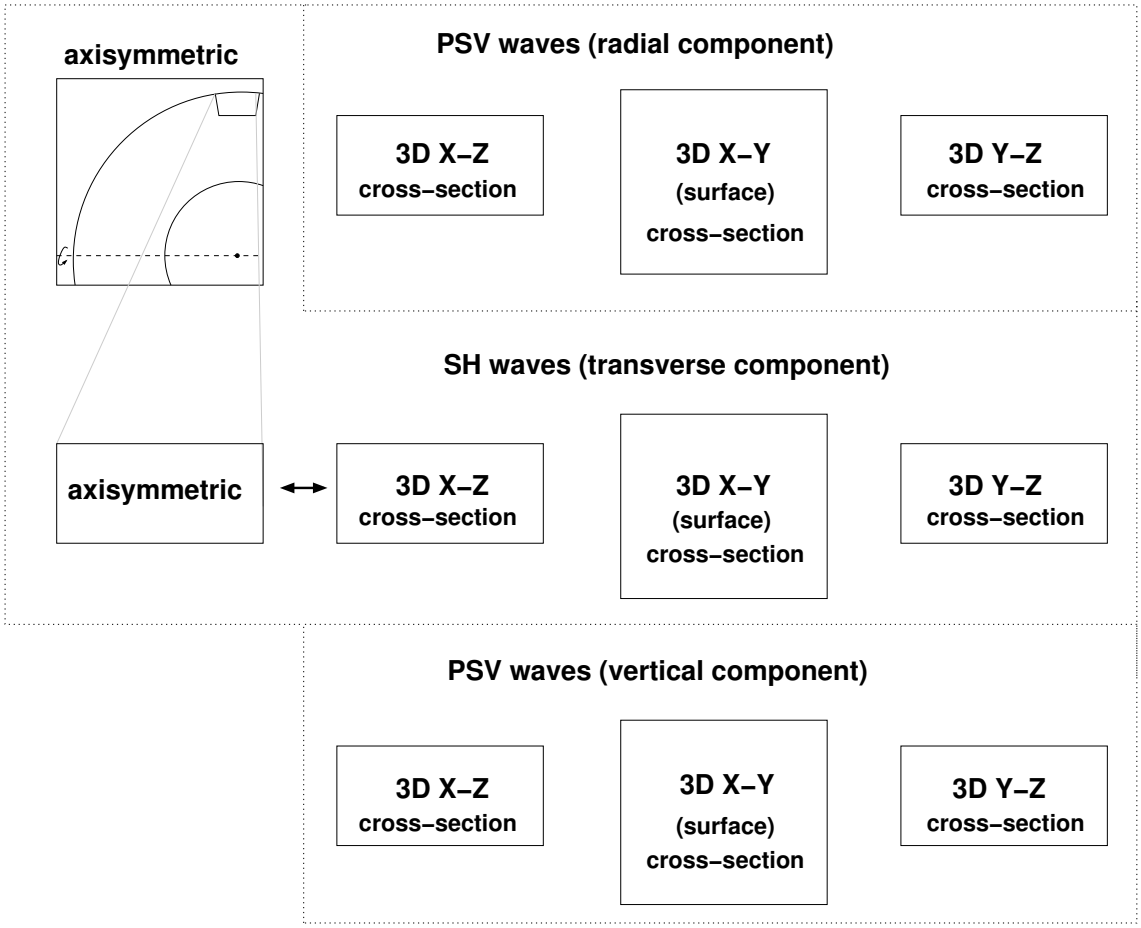

Figure 6: Legend to the snapshot figures of the hybrid code. In the upper left the SH wavefield of the axisymmetric domain is shown together with the symmetry axis and the position of the 3-D section. Below, the axisymmetric wavefield at the position of the 3-D section is enlarged. To the right of that, the wavefield at the same position, but calculated with the 3-D code is shown. Differences between these wavefield should be only due to the usage of different models in the two codes (e.g. PREM in the axi-symmetric and PREM+plume in the 3-D domain). The other images in the middle row are other cross-sections through the model, all showing the transverse (SH) component. The upper and lower row show the radial and vertical components, respectively. Both components contain PSV waves and since no PSV energy is fed in by the axi-symmetric code, these can only been generated by conversions due to lateral heterogeneities in the 3-D. model. The right column shows depth cross-sections perpendicular to the direction of wave propagation, the middle column shows surface cross-section, and the left one shows depth cross-sections in the direction of wave propagation, as the leftmost column does for the axi-symmetric wavefield.

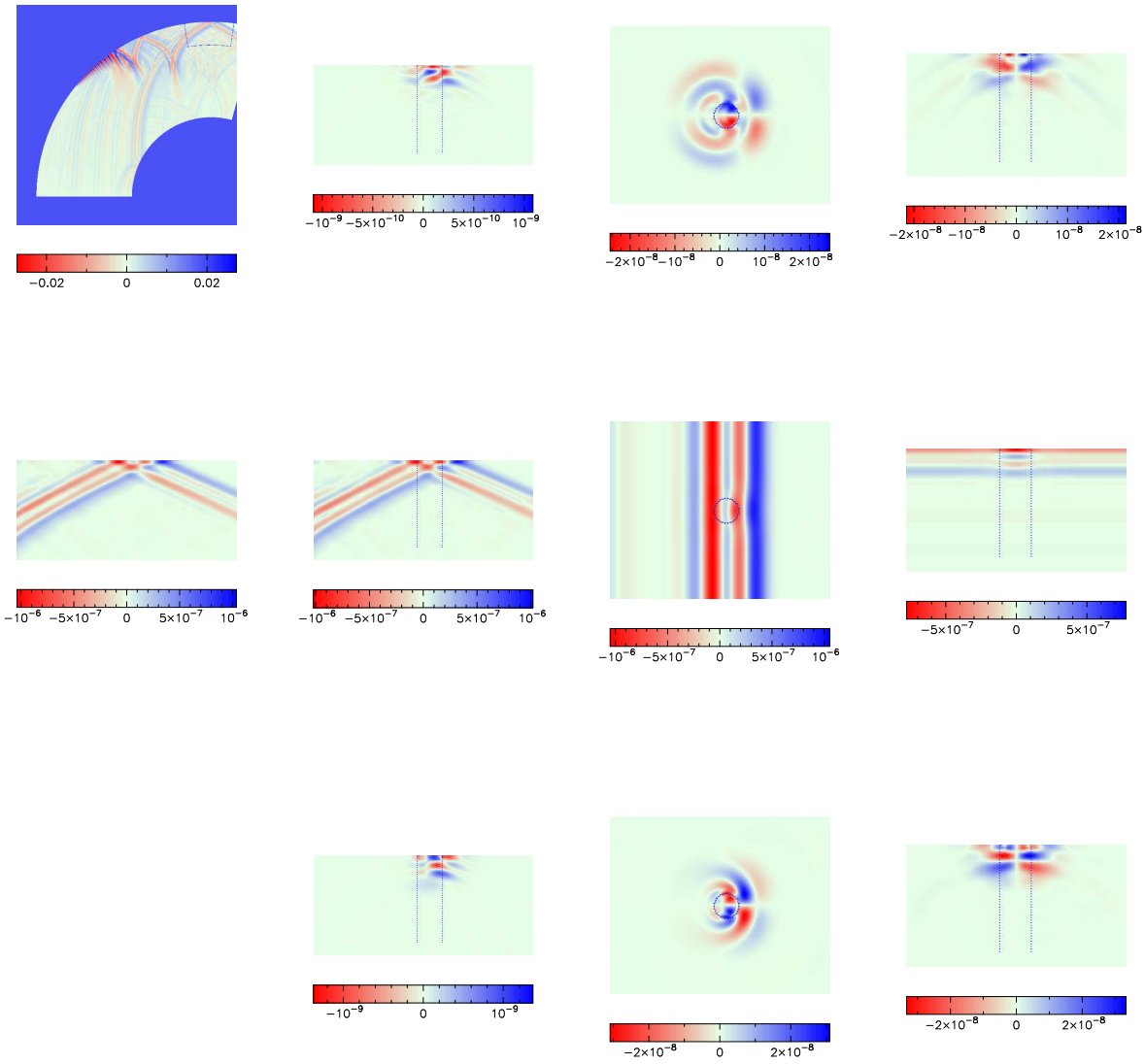

Figure 7: Snapshots of the wavefield as calculated with the hybrid code. A legend for this figure is given in fig. 6. The upper and the lower row show conversions caused by the plume. In the middle picture (surface SH-motion) the healing behind the plume is clearly visible. Absolute amplitudes are arbitrary and serve only for comparison. Plume boundaries are given in blue.

The panels of figure 7 show snapshots of the wavefield at different cross-sections (for a legend see fig. 7) through the plume center (horizontal depth slices or at the surface) of the three components (radial, transverse and vertical). Since only SH waves are fed in from the axisymmetric code only the middle row (showing transverse, i.e. SH motion) gets a signal. Motions on the other components are due to conversions at the plume. Conversion seismograms are shown in fig. 8, for both the vertical (subfigure (a)) and the radial component (b). In these figures the arrival times of the SH wave are marked as black lines. The conversions concentrate in the epicentral distance range of the plume (cf. TILMANN *et al.* [1998]) and behind it. Note also some converted signals before the arrival of the original SH-wave (e.g. at 90°). This is due to conversion at greater depth and subsequent faster propagation of the generated P wave. The two leftmost panels of the middle row in fig. 7 show the transverse (SH) component of the axisymmetric domain (left) and the spherical section. They differ only slightly, this is the difference in the wavefield caused by the plume.

Compared to other methods the parallel computation of the axisymmetric wavefield with the 1D model along with the wavefield in the spherical section using a 3-D model has the advantage that the undisturbed solution is always provided along with the seismograms that are influenced by the 3D structure. A separate run for the background model (which is 1D) alone, neede for comparison, is an overkill to the problem, when carried out in full 3D.

Parallelization

In order to achieve high-frequent wavefield simulations, workstation clusters or supercompusters have to be used which requires parallel algorithms. The concept for parallelizing the hybrid algorithm goes beyond simple classical FD domain decomposition and is presented in the following.

Parallelization using domain decomposition and the Message Passing libraries (MPI) is currently the standard way to obtain reasonable portability and performance of numerical wave propagation codes even if the extra effort for parallelization is significant.

For the hybrid code a parallelization scheme based on MPI has been developed (fig. 9). Apart from running the parallelized subcodes in parallel inter-code communication is necessary. As a result of a long line of development and testing a scheme was developed that takes advantage of the the possibility to define groups of processes within MPI, each with its own communicator (e.g. `MPI_COMM_SH` in fig. 10).

Thus, it is possible to create a separate environment for each of the codes in a way such that there is no interference of the codes for example if the same variable names are used in the codes. This is an advantage since it allows development of the subcodes without much consideration of the other codes, as long as the variables used for inter-code communication are not affected.

Between these environments inter-code communication is possible using the global message-passing communicator (`MPI_COMM_WORLD`). However, the development of the routines that pass the axi-symmetric wavefield to the spherical section was the most time consuming task since domain sizes of the individual codes differ in general. The concept of the resulting hybrid communication scheme is shown in 10. It was implemented and tested on the Institute's Linux workstation cluster, and then, for production runs, transferred to the Bundeshöchstleistungsrechner (Hitachi SR-8000) at the Leibnitz-Rechenzentrum.

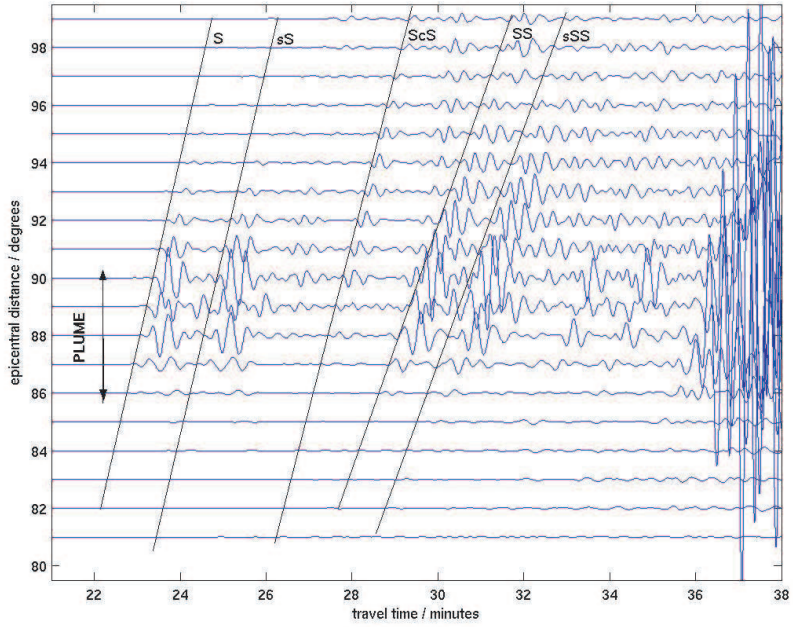

(a) vertical component

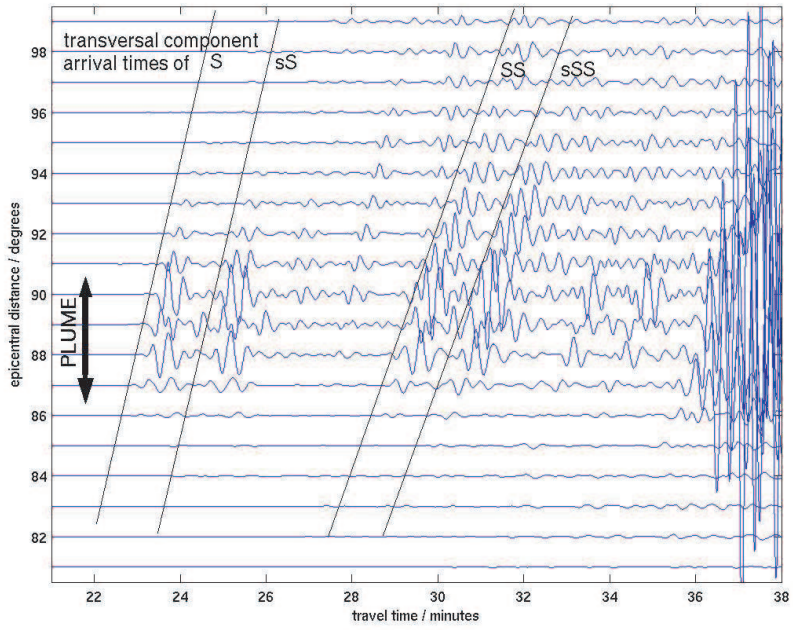

(b) radial component

Figure 8: SH to PSV Conversions caused by the plume. a) close up of radial component, b) vertical component. When feeding the spherical section only with SH waves, a signal appearing on the radial and vertical components can only result from conversions of SH to P-VS waves by a lateral heterogeneity, i.e. the plume. The onsets of some SH-phases are given as a black line, for reference. Note that some of the P-VS onsets here are earlier than these SH-arrivals, because P-waves travel faster after conversion than SH waves.

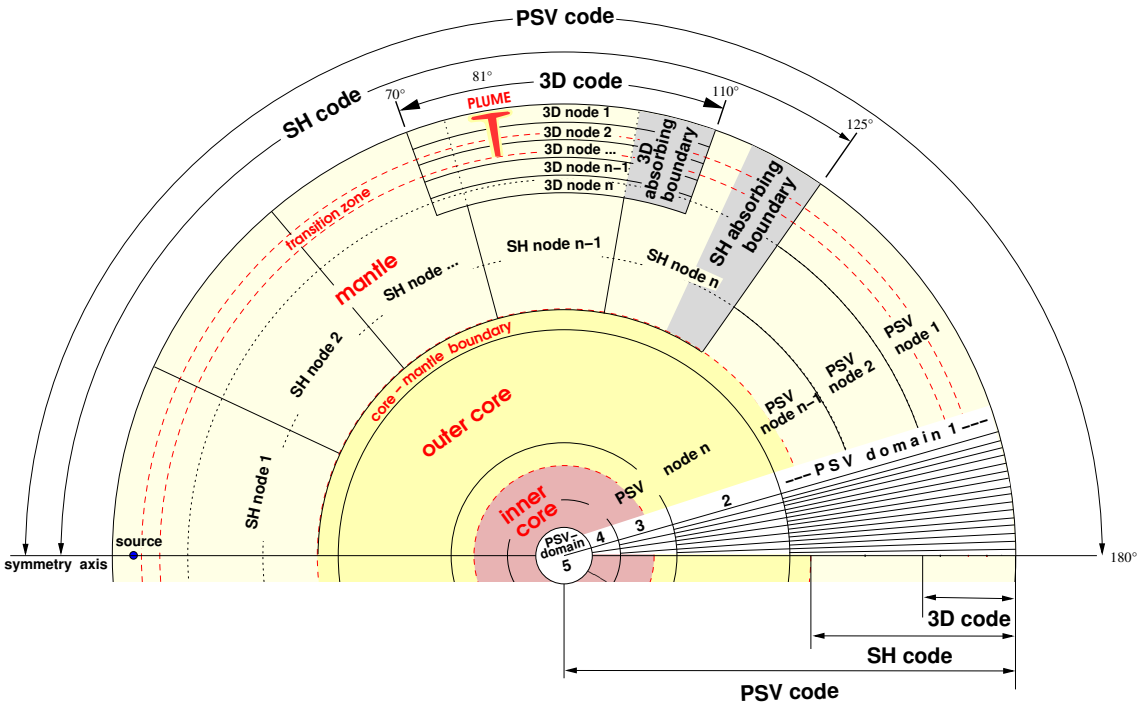

Figure 9: The complete parallelization scheme of the hybrid code with the axi-symmetric SH- and PSV code and the 3-D spherical section code. The PSV-code uses m nodes and covers the entire epicentral range (0-180°), with a vertical domain decomposition and a vertical, but different parallel distribution of nodes. The SH-code only covers an epicentral range that in this example slightly exceeds the 3D section's back end (0-125°). It is parallelized in the θ-direction and uses n nodes. The 3D spherical section (here, 70-110°) again uses vertical parallelization with k nodes. As an example, a plume coming from the '660' is implemented at an epicentral distance of 81°. Major discontinuities of the Earth are given in red dotted lines, node or domain boundaries in black. Grey shaded regions are the absorbing boundaries of the SH and the 3D code. At the right side at high epicentral distances the grid is shown with the domain numbers for the PSV-code.

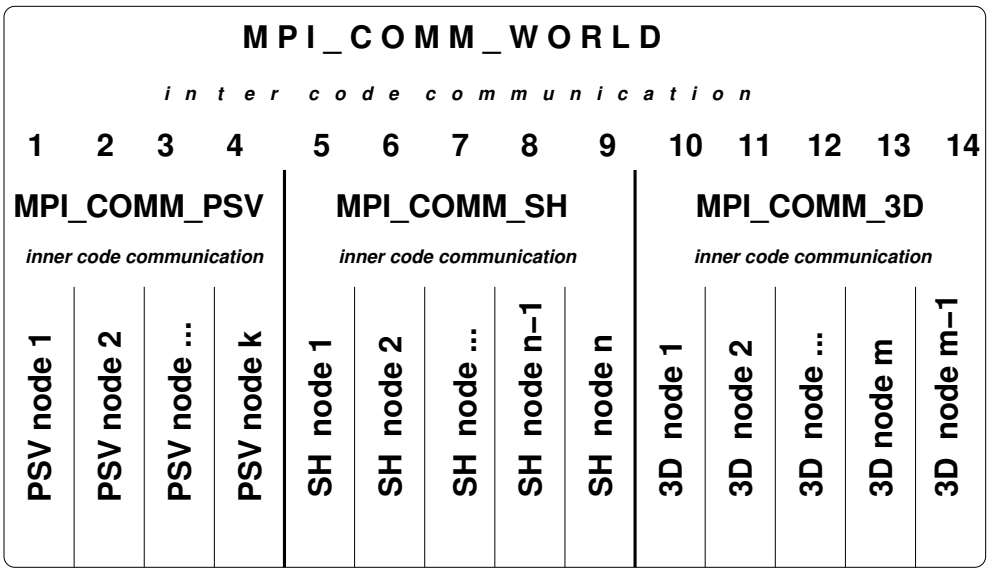

Figure 10: The hybrid communication concept. In this example, 12 nodes are globally available for the hybrid code (global node numbering from 0-11). The global MPI-communicator MPI-COMM-WORLD enables communication between all the nodes, and thus also inter-code communication. The nodes are distributed on the different codes. For each code a MPI sub-group for inner-code communication is set up, as well as node numbering for each code.

Discussion

To study 3-D wavefield effects of spatially confined structures in the mantle such as slabs or plumes an accurate modeling of 3-D wave propagation is necessary. However, full 3-D methods, though available and more and more used (e.g. KOMATITSCH AND TROMP [2002]) are computationally still very expensive and are an overkill to the problem since most of the Earth structure modeled is still only 1-D. In this study, we present a hybrid method that combines an axisymmetric approach with a spherical section method. In this method the propagation of the wavefield over the long epicentral distance range is modeled using a 2-D computational domain allowing for an efficient computation with an axi-symmetric or 1-D (e.g. PREM) background model. Around the structure of interest, the global wavefield is passed to a confined 3-D spherical section grid, on which the full 3-D wavefield including the interaction with the modelled structure is computed. An advantage is, that the expensive calculation in the 3-D domain is only activated when energy approches the 3-D section, which saves computation time.

This setup is ideally suited for parameters studies with a lot of parameter combinations for confined structures and their interaction with the global wavefield at teleseismic distances. For closer distances the spherical section code can be used alone. Moreover, the hybrid method benefits from the possibility of considerung only one of the independent wavefields (SH or PSV) due to their decoupling for axisymmetric models as used. Thus, the study of conversions (SH to PSV and vice versa) is possible with the advantage to obtain the converted signals alone and not mixed with the actual signals on the respective component.

We have shown that with this method a 3-D wavefield study is feasible on a desktop PC that would require a 150 processor supercomputer for the same frequency and full 3-D calculation. For the time until full 3-D calculations are feasible with an effort that allows for mass calulations the hybrid method presented here might be a helpful tool for parameters studies of confined structures in the Earth's mantle.

Acknowledgements

We thank the Leibniz-Rechenzentrum in Munich for the access to their supercomputers. This work was partly funded by the Deutsche Forschungsgemeinschaft (projects Ig16/2 and Ig16/4).

References

CAPDEVILLE, Y., E. CHALJUB, J. P. VILOTTE and J. P. MONTAGNER. *Coupling the spectral element method with a modal solution for elastic wave propagation in global earth models.* Geophys. J. Int., volume 152: 34–67, **2003**.

CAPDEVILLE, Y., C.LARMAT, J.-P. VILOTTE and J.-P. MONTAGNER. *A new coupled spectral element and modal solution method for global seismology: A first applictaion to the scattering induced by a plume-like anomaly.* Geophys. Res. Lett., volume 29(9): 31–1 – 32–4, **2002**.

CAPDEVILLE, Y., E. STUTZMANN and J. P. MONTAGNER. *Effect of a plume on long period surface waves computed with normal modes coupling.* Phys. Earth Planet. Inter., volume 119: 57–74, **2000**.

CHALJUB, E. *Modélisation numérique de la propagation d'ondes sismiques en géométrie sphérique : application à la sismologie globale*. Ph.D. thesis, Université Denis Diderot, Paris VII, **2000**.

CHALJUB, E. and A. TARANTOLA. *Sensitivity of SS precursors to topography on the upper-mantle 660-km discontinuity*. Geophys. Res. Lett., volume 24: 2613–2616, **1997**.

CHAPMAN, C. H. *A new method for computing synthetic seismograms*. Geophys. J. R. astr. Soc., volume 140: 81–85, **1978**.

DZIEWONSKI, A. and D. ANDERSON. *Preliminary Reference Earth Model*. Phys. Earth Planet. Inter., volume 25: 297–356, **1981**.

FUCHS, K. and G. MÜLLER. *Computation of synthetic seismograms with the reflectivity method and comparison with observations*. Geophys. J. R. astr. Soc., volume 23: 417–433, **1971**.

IGEL, H. *Seismic Modelling and Inversion*. Ph.D. thesis, Université Paris 7, **1993**.

IGEL, H. and O. GUDMUNDSSON. *Frequency-dependent effects on travel times and waveforms of long-period S and SS waves*. Phys. Earth Planet. Inter., volume 104: 229–246, **1997**.

IGEL, H., T. NISSEN-MEYER and G. JAHNKE. *Wave propagation in 3D spherical sections: Effects of subduction zones*. Phys. Earth Planet. Inter., volume 132: 219–234, **2002**.

IGEL, H., N. TAKEUCHI, R. GELLER, C. MÉGNIN, H.-P. BUNGE, E. CLÉVÉDÉ, J. DALKOLMO and B. ROMANOWICZ. *The cosy Project: verification of global seismic modeling algorithms*. Phys. Earth Planet. Inter., volume 119: 3–23, **1999**.

IGEL, H. and M. WEBER. *SH-wave propagation in the whole mantle using high-order finite differences*. Geophys. Res. Lett., volume 22: 731–734, **1995**.

IGEL, H. and M. WEBER. *P-SV wave propagation in the Earth's mantle using finite differences: Application to heterogeneous lowermost mantle structure*. Geophys. Res. Lett., volume 23(5): 415–418, **1996**.

JAHNKE, G. *Numerical modeling of seismic wave propagation: fault zones and global earthquakes (in preparation)*. Ph.D. thesis, Ludwig-Maximilians-Universität München, **2005**.

JAHNKE, G., T. NISSEN-MEYER, M. TREML and H. IGEL. *High Resolution Global Wave Propagation for Axi-Symmetric and additional 3D Geometries*. EGS XXVII General Assembly, Nice, 21-26 April 2002, abstract #4580, volume 27: 4580–+, **2002**.

KENNETT, B. L. N. and E. R. ENGDAHL. *Traveltime for global earthquake location and phase identification*. Geophs. J. Int, volume 105: 429–465, **1991**.

KENNETT, B. L. N., E. R. ENGDAHL and R. BULAND. *Constraints on seismic velocities in the Earth from travel-times*. Geophys. J. Int., volume 122(1): 108–124, **1995**.

KOMATITSCH, D. and J. TROMP. *Spectral-element simulations of global seismic wave propagation — I. Validation*. Geophys. J. Int., volume 149: 390–412, **2002**.

Moczo, P., J. Kristek and L. Halada. *The Finite-Difference Method for Seismologists. An Introduction.*. Comenius University, Bratislava, **2004**. ISSN 80-223-2000-5.

Moczo, P., J. O. A. Robertsson and L. Eisner. *The finite-diference time-domain method for modelling of serismic wave propagation.* In: R. Dmowska (editor), *Adavnaces in Wave Progagtion in heterogeneous Earth*, Advances in Geophysics. Elsevier Academic Press, **2006**.

Nissen-Meyer, T. *Numerical Simulation of 3-D Seismic Wave Propagation through Subduction Zones.* Diplomarbeit, Ludwig-Maximilians-Universität München, **2001**.

Strasser, M. *Numerical modeling of 3D wave effects of plumes.* Diplomarbeit, Ludwig-Maximilians-Universität München, **2001**.

Thomas, C., H. Igel, M. Weber and F. Scherbaum. *Acoustic simulation of P-wave propagation in a heterogeneous spherical Earth: numerical method and application to precursor waves to PKPdf.* Geophys. J. Int., volume 141: 307–320, **2000**.

Tilmann, F. J., D. McKenzie and K. F. Priestley. *P and S wave scattering from mantle plumes.* J. Geophys. Res., volume 103(B9): 21, **1998**.

Tromp, J., C. Tape and Q. Liu. *Seismic tomography, adjoint methods, time reversal, and banana-doughnut kernels.* Geophys. J. Int., **2005**.

Virieux, J. *P-SV wave propagation in heterogeneous media: Velocity-stress finite-difference method.* Geophysics, volume 51(4): 889–901, **1986**.

Wen, L. *An SH hybrid method and shear velocity structures in the lowermost mantle beneath the central Pacific and South Atlantic Oceans.* J. Geophys. Res., volume 107(B3): ESE 4–1 – ESE 4–20, **2002**.

Wen, L. and D. V. Helmberger. *A 2-D P-SV hybrid method and its application to modeling localized structures near the core-mantle boundary.* J. Geophys. Res., volume 103: 17 901–17 918, **1998**.